NASA
Technical
Paper
2596

May 1986

Velocity Profiles in Laminar Diffusion Flames

Valerie J. Lyons
and Janice M. Margle

NASA

NASA Technical Paper 2596

1986

Velocity Profiles in Laminar Diffusion Flames

Valerie J. Lyons
Lewis Research Center
Cleveland, Ohio

Janice M. Margle
Pennsylvania State University
Abington, Pennsylvania

NASA
National Aeronautics
and Space Administration

Scientific and Technical Information Branch

Summary

Velocity profiles in vertical laminar diffusion flames were measured by using laser Doppler velocimetry (LDV). Four fuels were used: *n*-heptane, iso-octane, cyclohexane, and ethyl alcohol. The velocity profiles were similar for all the fuels, although there were some differences in the peak velocities. The data compared favorably with the theoretical velocity predictions. The differences could be attributed to errors in experimental positioning and in the prediction of temperature profiles. Errors in the predicted temperature profiles are probably due to the difficulty in predicting the radiative heat losses from the flame.

Introduction

The purpose of this investigation is to further characterize the flow field of a vertical boundary-layer laminar diffusion flame. The well-established nature of this flow allows analytical predictions of the flow velocities to be compared with data obtained from the present study. A schematic of the flow is given in figure 1. Shown is a vertical wall which contains a wick made of a porous material soaked with liquid fuel. When the wick is ignited, a vertical boundary-layer flame is formed which is composed of several regions. The region nearest the wall is the pyrolysis zone, where the fuel vaporizes and begins to break down. The next region out from the wall is the soot layer, where rich burning produces the soot particles that are typical of incomplete combustion. Next is the flame zone, a thin region where the temperature is a maximum. Outside the flame zone the fuel is almost completely burned. The boundary-layer edge is shown between the region containing gases which are influenced by the flame and the region of ambient, still air. The coordinate system used is also shown, where x is the streamwise coordinate measured from the leading edge of the wick, and y is the coordinate measured from the wall, across the flow. This configuration is well documented in the literature (refs. 1 to 3) and has been of particular interest in the study of sooting laminar diffusion flames (refs. 4 and 5). The presence of soot in a flame influences radiative heat transfer. This may be undesirable (e.g., in a combustion chamber of an engine or in a compartment fire) or desirable (e.g., in a furnace). Since temperature and velocity control soot transport in a flame, a better understanding of these parameters should lead to better designs of systems that require consideration of radiative heat transfer caused by soot in a flame.

The exact mechanism of soot formation, growth, and destruction is not fully understood. It is necessary to study the overall flow-field parameters to learn their effects on soot before the microscopic details can be studied. Beier and Pagni (ref. 4) measured soot concentration profiles as well as temperature profiles in a vertical boundary-layer diffusion flame that was identical to the one used in the present study. The purpose of the present study was to measure velocity profiles within a vertical boundary-layer flame by using nonintrusive laser Doppler velocimetry (LDV). This information would verify the theoretical predictions of the velocity profiles in this flame and would give further understanding of the rate of propagation of soot particles in the flow. This could shed some light on the growth and destruction of soot particles through better understanding of their transport in the flame.

First developed to measure velocities in cold flows, LDV has grown to be a common tool for measuring flow velocities in many difficult flow fields, including combusting flows. The basic principle of LDV is that a laser beam is split into two beams of equal intensity which are then crossed to form a probe volume in which light and dark interference fringes occur. When a seed particle passes through the probe volume and crosses the fringe pattern, it scatters light, which is picked up by a photodetector. The photodetector senses a signal the frequency of which is proportional to the particle velocity. See reference 6 for more details. Examples of LDV research which involve combustion can be found in references 7 to 9, which represent only a small portion of the large body of literature that is available. Combusting flows offer an additional challenge to measurements using LDV since it is necessary to seed the flow with particles which follow the flow, scatter light, but do not burn up.

Apparatus and Procedure

The burner used in this study is shown schematically in figure 2. The burner consisted of a 50- by 75- by 25-mm ceramic fiberboard wick inserted into a 150- by 75- by 25-mm recess in a 450- by 550- by 25-mm vertical Marinite (fireproof) board. A 50- by 75- by 25-mm Marinite piece was used to hold the wick in place and to allow easy wick removal for refueling.

Velocity was measured at 0.5-mm increments in the horizontal, or y, direction and at two elevations in the vertical, or x, direction. In the vertical direction velocity was measured at heights of 20 and 40 mm from the bottom edge of the wick. These two x-direction settings were made by raising (or lowering) the burner with four large adjusting screws, which were also used to level the burner. In the horizontal direction, the burner was positioned by using a finely threaded rod. The 0.5-mm increments were measured with a digital micrometer accurate to 0.01 ± 0.005 mm.

The experimental apparatus is shown schematically in figure 3. The LDV system consisted of a 2-W argon-ion laser, transmitting and receiving optics, and a photodetector. The transmitting optics split the laser beam into two beams of equal intensity, separated them, and then focused and crossed them to create the probe volume in the flame. The receiving optics received the light scattered from particles passing through the probe volume and focused it onto the photodetector. The Doppler signal from the photodetector was sent to a counter-type signal processor and then was examined for visibility and strength by using an oscilloscope. The counter-type signal processor was used to convert the analog frequency signal to a digital representation of the time of flight of a particle passing through a desired number of fringes. This time of flight is inversely proportional to particle velocity (ref. 10). All the particle velocities were stored as velocity histograms in the minicomputer. See table I for details of the components of the LDV system.

The signal was very weak in the backscatter mode, so that it was necessary to add a collimating lens and a corner cube (as shown in fig. 3) to simulate a forward-scatter setup. This arrangement reflected the laser light back on itself, so that the particles scattered this reflected light in the same fashion as a forward-scatter LDV system. This increased the signal strength significantly. The arrangement was recommended by Rajan Menon of TSI Incorporated.

TABLE I.—LDV COMPONENT SPECIFICATIONS

[Argon-ion 2-W laser.]

Wavelength of laser light, μm	0.5145
Beam diameter (at $1/e^2$ points before expansion), mm	1.3
Beam separation distance, mm	22
Beam expansion ratio	3.75
Transmitting/receiving lens focal length, mm	480
Fringe spacing, μm	3.00
Number of fringes	28
Probe volume diameter, μm	84
Collimating lens focal length (for corner cube), mm	190
Beam half-angle, deg	4.91
Number of cycles per burst	8
Counter operating mode	Single burst

The seed-particle generator used was a fluidized-bed type that seeded the flow with aluminum oxide particles having a mean diameter of 1 μm. The relatively low velocity of the flame made it difficult to find a seeding technique that would not interfere with the flow. Small, high-flow-velocity fluidized-bed particle generators blew out the flame even with attempts to diffuse the seed flow. The most successful seeding technique used a very large seed generator (450-liter/min, 10- to 100-mg/m^3 mass output; 10^5 particles/cm^3). The burner was surrounded by a Plexiglas enclosure with an exhaust hood. (The exhaust fan was used after each run to clear the combustion products and turned off before the seed particles were introduced.) The ceramic fiberboard wick was soaked with liquid fuel until saturated. It was then positioned in the Marinite wall at the far right side of the recess and held in place with the Marinite spacer. For the data taken at the $x = 40$ mm position, the burner was ignited, and then the enclosure was filled with a cloud of aluminum oxide particles from the seed generator. The flame was allowed to stabilize so that it was visibly smooth before data were taken. At the $x = 20$ mm position, the boundary layer was thinner and had less outside air entrainment, which made it more difficult to seed. Therefore it was necessary to fill the enclosure with seed first, then to light the flame so that more seed particles were in the flow immediately. The flame stabilized more quickly by using this approach, which allowed data to be taken before the seed particles settled out of the ambient air.

The method used to determine the distance y from the wall was to begin a series of measurements near the boundary-layer edge (near y = nominally 7 mm). Measurements were then taken at 0.5-mm increments until the wall blocked the incoming laser beams and would not allow further measurements. An estimate of the location of this limiting value of y was obtained in the following manner. The laser beam was expanded by the LDV optics to 4.875 mm in diameter ($1/e^2$ intensity). The beam was then focused to a diameter of 84 μm in the probe volume, 480 mm from the output lens of the LDV system. The left edge of the Marinite wall was 194 mm from the output lens. The laser beam was approximately 2 mm in diameter when it first came in contact with the edge of the Marinite wall, so that the center of the beam (the location of the probe volume) was 1 mm from the wall. This value of 1 mm was used as the y location of the first data point from the wall for all the profiles measured.

Results

Velocities were measured in flames produced by burning four fuels: ethyl alcohol (absolute), iso-octane (2,2,4-trimethylpentane, reagent grade), cyclohexane (hexahydrobenzene, reagent grade), and n-heptane (distilled in glass). The velocity measurements in the laminar diffusion flames were plotted as velocity histograms. A typical velocity histogram is shown in figure 4(a) for iso-octane fuel at $y = 5$ mm

from the wick surface and $x = 40$ mm from the leading edge of the wick. The mean velocity is 86.86 cm/sec, and the standard deviation from the mean is 4.68 percent for the 2000 data points taken. These results show that the flow was fairly steady. An example of a poor histogram taken at the same location is shown in figure 4(b). The mean velocity is not the same as in figure 4(a), and the standard deviation is also higher (13.6 percent). The higher standard deviation is most likely due to unsteady effects, seen as flickering of the flame as the fuel supply runs low. This was more likely to occur during longer sampling times, which were required when the seeding was sparse. Attempts were made to acquire data with the lowest possible standard deviation. The number of data points recorded seemed to have little effect. As shown in figures 5(a) and (b), for nearly the same (high) standard deviation, the mean velocity is nearly the same (98.6 and 98.3 cm/sec) for 1000 and 500 data points. This is also shown for a lower standard deviation, in figures 6(a) and (b), where 500 and 250 data points produced nearly the same mean velocity (97.9 and 95.2 cm/sec).

The mean velocities from these histograms are plotted as functions of position as measured horizontally from the fuel-wick surface to produce the velocity profiles shown in figure 7. The closest measurable point is approximately 1 mm from the wick surface. Measurements closer to the wick were hampered because the wall blocked the incoming laser beams from the LDV system. Representative error bars shown on various data points mark the standard deviation about the mean velocity measurement. Bars are shown only on selected points for clarity.

In general, all velocity profiles had the same configuration. Profiles were low near the wall and when approaching the edge of the boundary layer, and they peaked somewhere within the boundary layer. These peaks occurred closer to the wall for the $x = 20$ mm case (nearer the boundary-layer leading edge) than for the $x = 40$ mm case. This was expected since the boundary layer is thinner at $x = 20$ mm. Also as expected the peak velocities are higher for the $x = 40$ mm case. In general, the downstream velocity ($x = 40$ mm) was greater than the upstream velocity ($x = 20$ mm) at nearly every horizontal location measured.

The effect of fuel type on the measured velocity profile is shown in figures 8 and 9. Least-squares cubic curve fits to the data are plotted for the two measurement locations. As shown in figure 8, the peak velocity at $x = 20$ mm was highest for ethyl alcohol (107.9 cm/sec). This fuel was followed by iso-octane (103.8 cm/sec), *n*-heptane (102.5 cm/sec), and cyclohexane (99.9 cm/sec). In figure 9, the peak velocities at $x = 40$ mm were higher than at $x = 20$ mm, but the fuel types remained in the same order: ethyl alcohol (136.8 cm/sec), iso-octane (132.3 cm/sec), *n*-heptane (130.8 cm/sec), and cyclohexane (125.2 cm/sec). Figures 8 and 9 also show that the peak velocities occurred at slightly different positions from the wall for the different fuels. At $x = 20$ mm, the fuel which produced a peak velocity closest to the wall was ethyl alcohol (4.17 mm). This was followed by *n*-heptane (4.25 mm), iso-octane (4.53 mm), and cyclohexane (5.04 mm). At $x = 40$ mm, the peaks occurred farther from the wall but in the same order with respect to fuel type: ethyl alcohol (5.32 mm), *n*-heptane (5.42 mm), iso-octane (5.46 mm), and cyclohexane (5.75 mm). A parabolic-least-squares curve fit was extrapolated to find the zero-velocity point and was used to define an experimental value for the boundary-layer thickness. At $x = 20$ mm, cyclohexane produced the thickest boundary layer (10.25 mm). This was followed by *n*-heptane (10.05 mm), ethyl alcohol (9.99 mm), and iso-octane (9.84 mm). At $x = 40$ mm, *n*-heptane (11.45 mm) was followed by ethyl alcohol (11.43 mm), cyclohexane (11.06 mm), and iso-octane (11.02 mm). All the fuels produced nearly the same boundary-layer thickness. This result was expected since their thermophysical properties are quite similar (ref. 5).

Discussion

Theoretical predictions of the velocity profiles in the boundary-layer flame are presented with the data in figures 10 to 12. The predictions that are presented in figures 10 to 12 were taken from reference 5. (There was no theoretical prediction for ethyl alcohol fuel). The mathematical model used describes a laminar boundary layer in which chemical reactions occur simultaneously with transfer of heat, mass, and momentum. Radiation heat loss is considered. Conservation equations for mass, momentum, species, and enthalpy (including a radiation flux term) are solved. A more complete description of the mathematical model can be found in reference 5.

As shown in figures 10 to 12, the data agree very well with the mathematical-model predictions at the $x = 20$ mm position for the entire velocity profile. The agreement is especially good for iso-octane, as shown in figure 12. The exact position of the laser probe volume from the wall was very difficult to determine precisely, and this could account for part of the difference between theory and data. At $x = 40$ mm, the model predicts somewhat higher velocities than were measured. This may be due in part to the flame-sheet approximation made in producing the theoretical temperature and velocity predictions. In a free-flow situation, the vertical velocity depends on the temperature, which determines the buoyancy force driving the flow. A flame-sheet approximation predicts a very sharply peaked temperature profile that would produce a higher peaked velocity profile.

As shown in table II, at $x = 40$ mm the following peak temperatures were predicted (ref. 11): 2235 K for iso-octane, 2245 K for cyclohexane, and 2240 K for *n*-heptane. The corresponding predicted peak velocities at the $x = 40$ mm location were 155.9 cm/sec for iso-octane, 152.4 cm/sec for cyclohexane, and 150.8 cm/sec for *n*-heptane. The temperature profiles measured by Ang, et al. (ref. 11) were lower than the theoretical predictions, and they also showed little variation

TABLE II.—COMPARISON OF PEAK TEMPERATURES AND VELOCITIES FOR SEVERAL FUELS

Fuel	Vertical distance, x, mm	Peak temperature, K		Peak velocity, cm/sec	
		Theory	Experiment	Theory	Experiment
Iso-octane	20	2240	2050	110	104
	40	2235	2050	156	132
Cyclohexane	20	2250	2060	108	100
	40	2245	2050	152	125
n-Heptane	20	2240	2080	107	103
	40	2240	2060	151	131

with respect to fuel type. Peak temperatures of 2060 K for n-heptane, 2050 K for iso-octane, and 2050 K for cyclohexane were measured at $x = 40$ mm. The fuel predicted to produce the lowest peak flame velocity was n-heptane. However, the velocity measurements show cyclohexane to have the lowest peak flame velocity. This was probably caused by the presence of soot in the flame. Since radiative heat transfer from the soot in the boundary-layer flame is not well understood, this could lead to temperature predictions that are higher than the actual flame temperatures. The measured soot volume fraction (ref. 5) for the n-heptane flame is much less (0.18 ppm) than for cyclohexane (0.31 ppm) or for iso-octane (0.40 ppm). Since increased soot loading increases radiative heat transfer, this could explain why the peak temperatures and velocities were lower for cyclohexane than for n-heptane. This may also explain why all the predicted velocity profiles at $x = 20$ mm show better agreement with the data than at $x = 40$ mm. As the flow moves downstream, the discrepancies in predicting radiative heat losses from the soot continue to widen the gap between theory and data.

Summary of Results

The velocity profiles in a vertical laminar diffusion flame were measured by using laser Doppler velocimetry (LDV). Four fuels were used: n-heptane, iso-octane, cyclohexane, and ethyl alcohol. Velocity profiles were quite similar for all the fuels. The main difference was in peak velocity. The highest peak velocity was obtained by using ethyl alcohol. This was followed by iso-octane, n-heptane, and cyclohexane.

The experimental data compared reasonably well with theoretical predictions. The small discrepancies observed were probably due to errors in experimental positioning and in the prediction of temperature profiles. Errors in the predicted temperature profiles were probably due to the difficulty in predicting the radiative heat losses from the flame and also due to the simplifying assumption of a flame-sheet approximation in the theoretical analysis.

Lewis Research Center
National Aeronautics and Space Administration
Cleveland, Ohio, March 3, 1986

References

1. Beier, R.A.; and Pagni, P.J.: Soot Volume Fraction Profiles in a Free Combusting Boundary Layer. ASME Paper 81-HT-1, Aug. 1981.
2. de Ris, J.: Fire Radiation—A Review. Seventeenth Symposium (International) on Combustion, The Combustion Institute, 1979, pp. 1003–1016.
3. Pagni, P.J.: Diffusion Flame Analyses. Fire Safety Journal, vol. 3, no. 4, Mar. 1981, pp. 273–285.
4. Beier, R.A.; and Pagni, P.J.: Soot Volume Fraction Profiles in Forced-Combusting Boundary Layers. J. Heat Trans., vol. 105, no. 1, Feb. 1983, pp. 159–165.
5. Beier, R.A.; Pagni, P.J.; and Okoh, C.I.: Soot and Radiation in Combusting Boundary Layers. Combust. Sci. Technol., vol. 39, no. 1-6, 1984, pp. 235–262.
6. Stevenson, W.H.: Principles of Laser Velocimetry. Experimental Diagnostics in Gas Phase Combustion Systems, B.T. Zinn, ed., AIAA, 1976, pp. 307–336.
7. Rambach, G.D.; Dibble, R.W.; and Hollenbach, R.E.: Velocity and Temperature Measurements in Turbulent Diffusion Flames. SAND-79-8775, Sandia National Labs, 1979.
8. Durst, F.; Melling, A.; and Whitelaw, J.H.: The Application of Optical Anemometry to Measurement in Combustion Systems. Combust. Flame, vol. 18, no. 2, Apr. 1972, pp. 197–201.
9. Durao, D.F.G.; and Whitelaw, J.H.: Critical Review of Laser Anemometry Measurements in Combusting Flows. Experimental Diagnostics in Gas Phase Combustion Systems, B.T. Zinn, ed., AIAA, 1976, pp. 357–376.
10. Laser Velocimetry Systems (Catalog). Form No. TSI LDV-879-23M-2MBRI, TSI Incorporated, St. Paul, MN, 1984.
11. Ang, J.A.; et al.: Temperature and Velocity Profiles in Sooting Free Convection Diffusion Flames. AIAA Paper 86-0575, Jan. 1986.

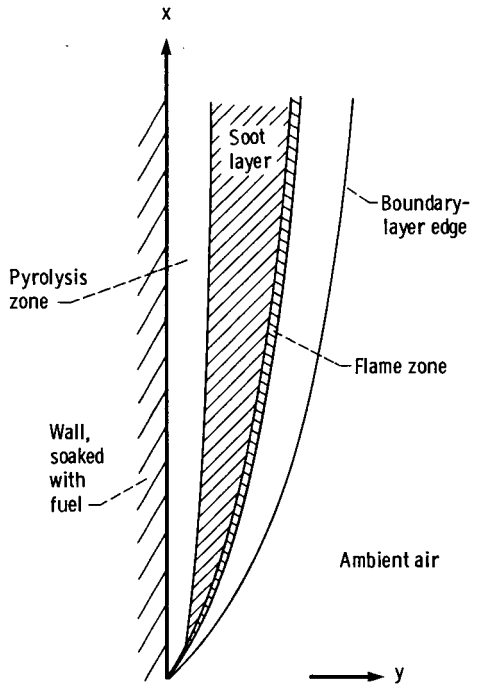

Figure 1.—Schematic of steady, buoyantly driven, two-dimensional, boundary-layer laminar diffusion flame on a vertical pyrolyzing fuel wall.

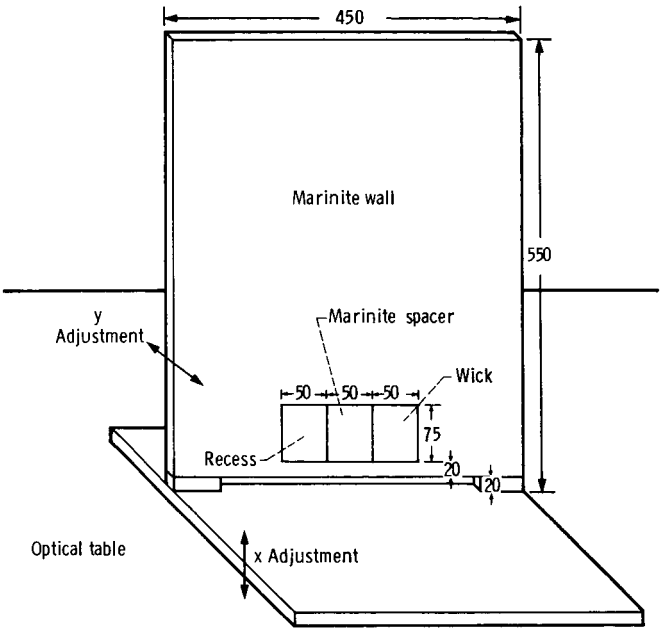

Figure 2.—Burner assembly. (All dimensions in millimeters.)

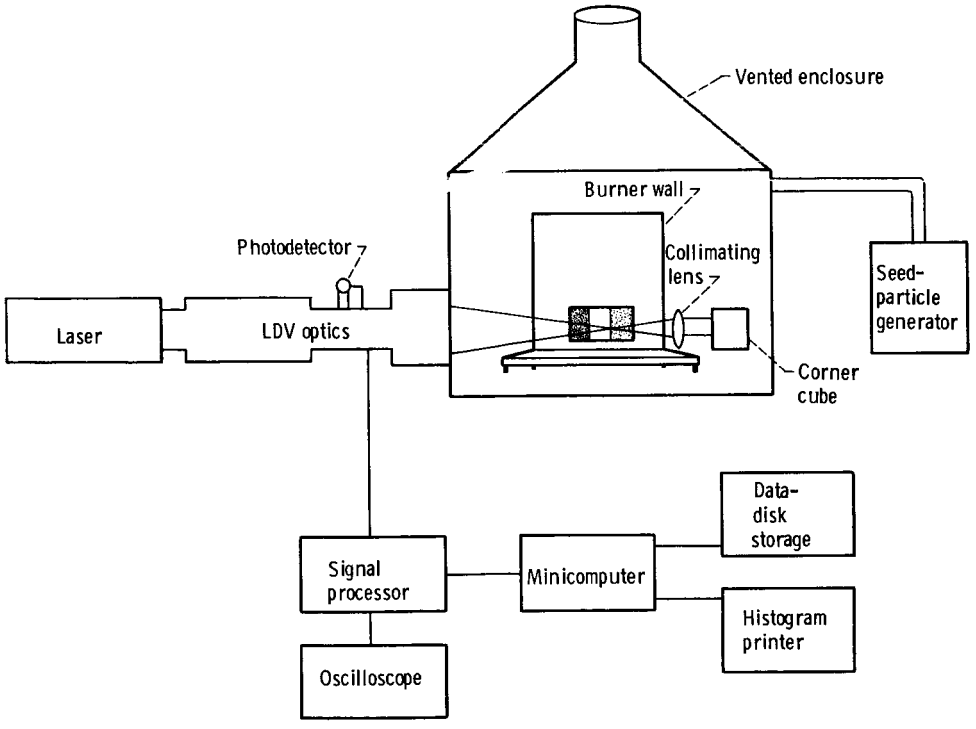

Figure 3.—Schematic of apparatus.

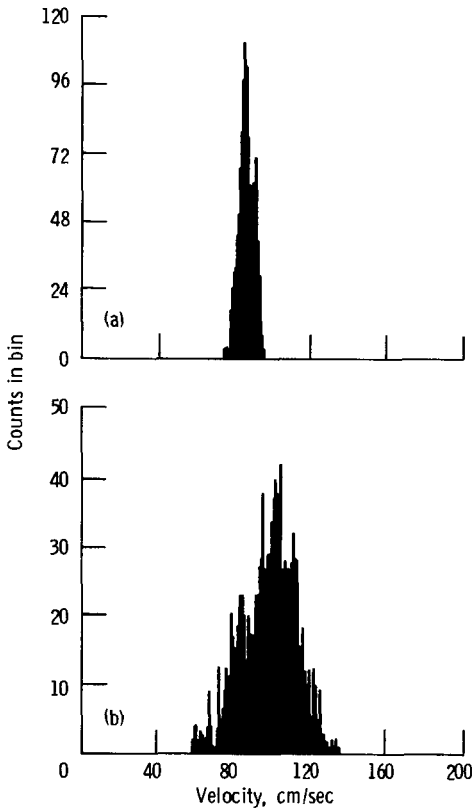

(a) Laminar diffusion flame. Data rate, 0.17015 kHz; mean velocity, 86.86 cm/sec; standard deviation, 4.68 percent.

(b) Flickering flame. Date rate, 0.15193 kHz; mean velocity, 100.15 cm/sec; standard deviation, 13.60 percent.

Figure 4.—Velocity histograms of 2000 data points for iso-octane. Ambient temperature, 25 °C (78 °F); ambient pressure, 0.986×10^5 N/m^2 (29.2 in. Hg); low limit, 30 kHz; high limit, 1000 kHz; x location, 40 mm; y location, 5 mm.

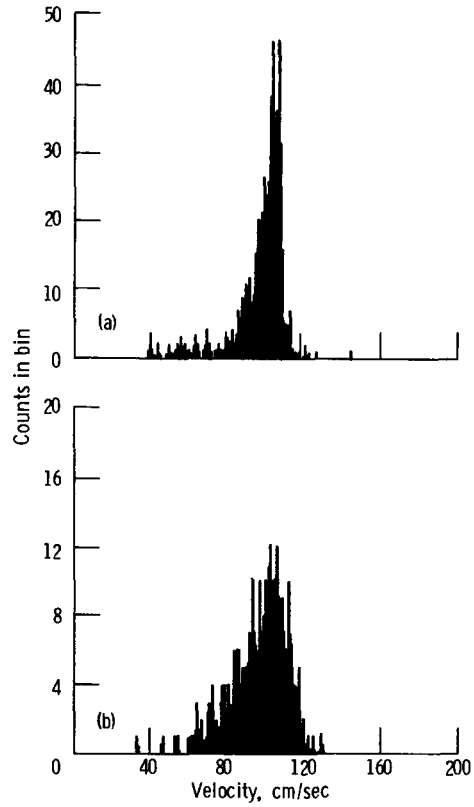

(a) For 1000 data points. Data rate, 0.00028 kHz; mean velocity, 98.60 cm/sec; standard deviation, 12.68 percent.

(b) For 500 data points. Data rate, 0.00036 kHz; mean velocity, 98.28 cm/sec; standard deviation, 13.38 percent.

Figure 5.—Velocity histograms for cyclohexane, high standard deviation. Ambient temperature, 22 °C (72 °F); ambient pressure, 0.999×10^5 N/m^2 (29.6 in. Hg); low limit, 3 kHz; high limit, 1000 kHz; x location, 20 mm; y location, 5 mm.

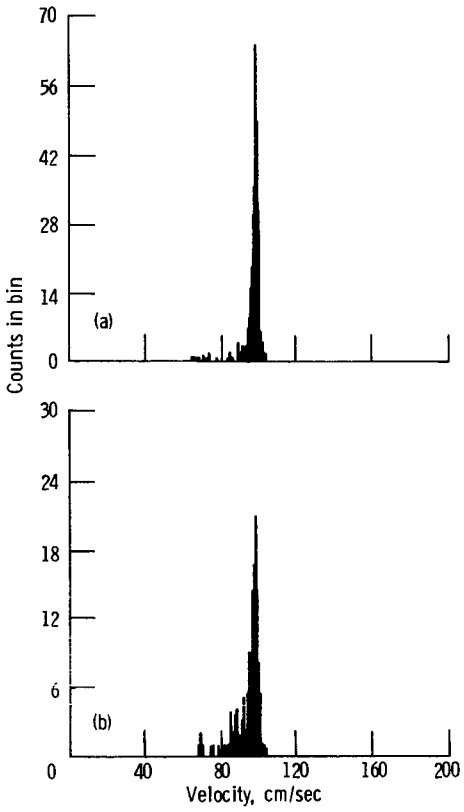

(a) For 500 data points. Data rate, 0.00013 kHz; mean velocity, 97.93 cm/sec; standard deviation, 4.46 percent.

(b) For 250 data points. Data rate, 0.00026 kHz; mean velocity, 95.18 cm/sec; standard deviation, 6.51 percent.

Figure 6.—Velocity histograms for cyclohexane, low standard deviation. Ambient temperature, 22 °C (72 °F); ambient pressure, 0.999×10^5 N/m^2 (29.6 in. Hg); low limit, 3 kHz; high limit, 1000 kHz; x location, 20 mm; y location, 2 mm.

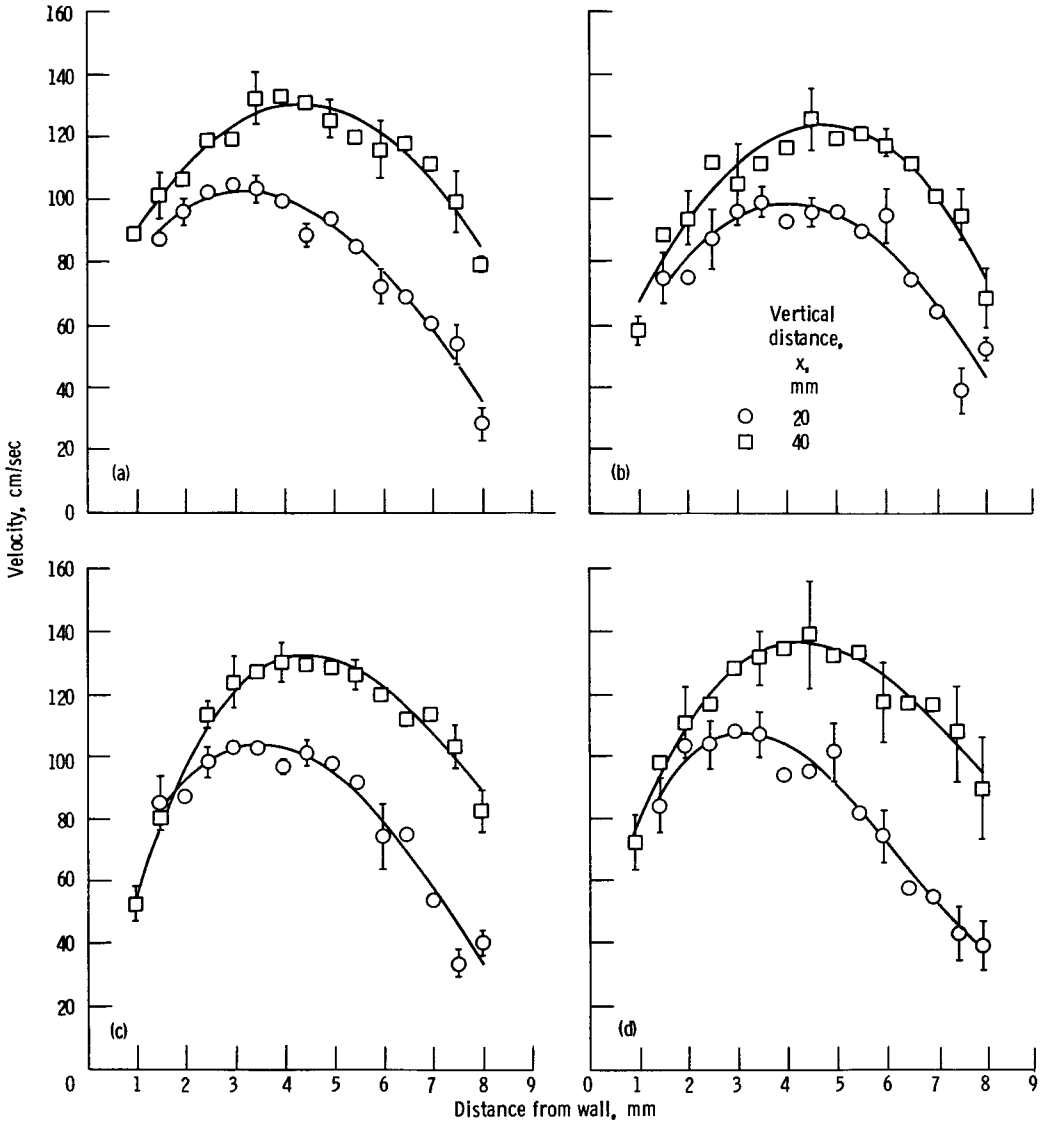

(a) *n*-Heptane.
(b) Cyclohexane.
(c) Iso-octane.
(d) Ethyl alcohol.

Figure 7.—Mean velocity as function of position for various fuels.

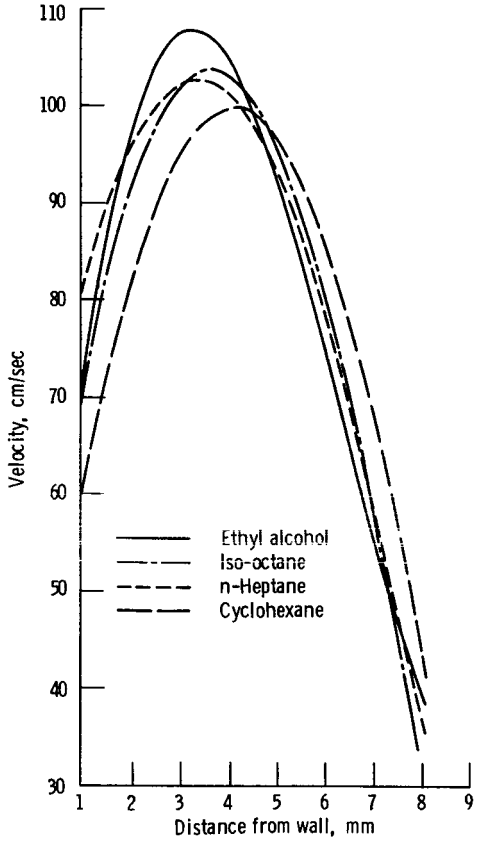

Figure 8.—Effect of fuel type on velocity at $x = 20$ mm.

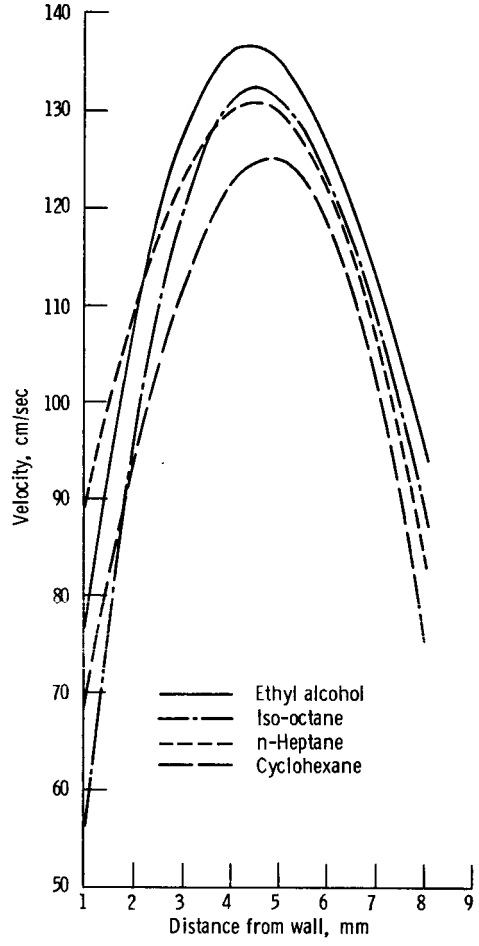

Figure 9.—Effect of fuel type on velocity at $x = 40$ mm.

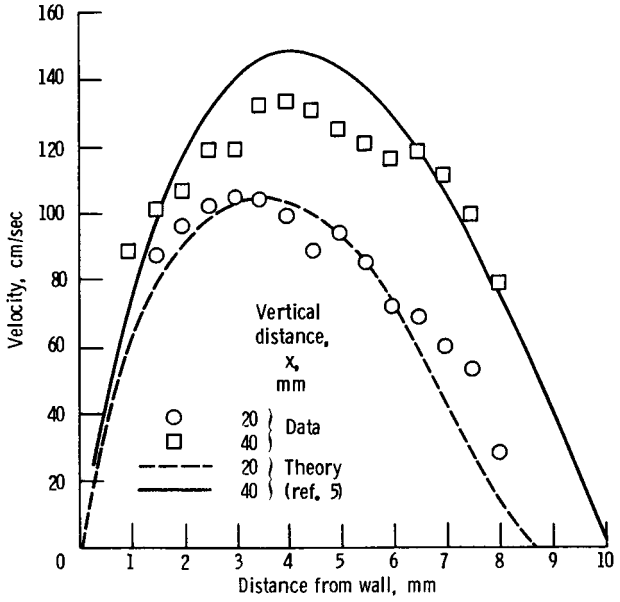

Figure 10.—Comparison of predicted and measured velocities for a vertical diffusion flame fueled by *n*-heptane.

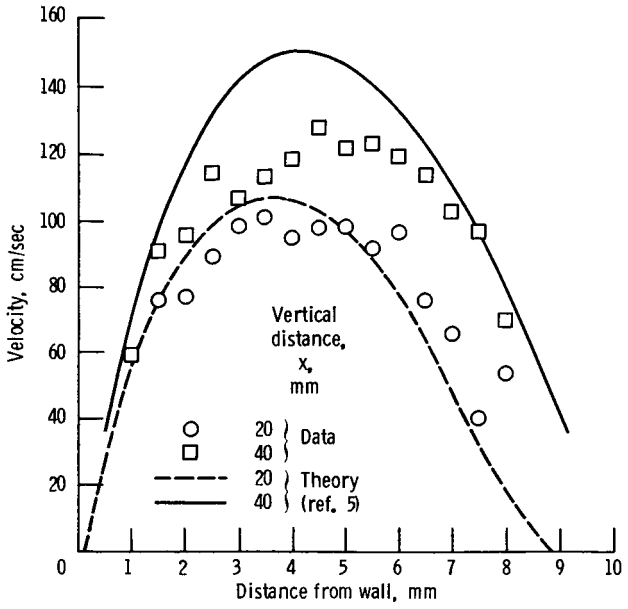

Figure 11.—Comparison of predicted and measured velocities for a vertical diffusion flame fueled by cyclohexane.

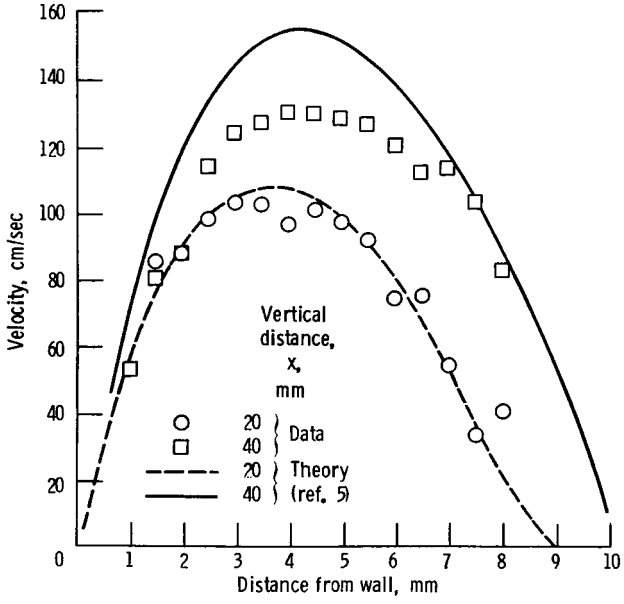

Figure 12.—Comparison of predicted and measured velocities for a vertical diffusion flame fueled by iso-octane.

1. Report No.	2. Government Accession No.	3. Recipient's Catalog No.
NASA TP-2596		

4. Title and Subtitle	5. Report Date
Velocity Profiles in Laminar Diffusion Flames	May 1986
	6. Performing Organization Code: 505-62-21
7. Author(s): Valerie J. Lyons and Janice M. Margle	8. Performing Organization Report No.: E-2879
	10. Work Unit No.
9. Performing Organization Name and Address: National Aeronautics and Space Administration, Lewis Research Center, Cleveland, Ohio 44135	11. Contract or Grant No.
	13. Type of Report and Period Covered: Technical Paper
12. Sponsoring Agency Name and Address: National Aeronautics and Space Administration, Washington, D.C. 20546	14. Sponsoring Agency Code

15. Supplementary Notes

Valerie J. Lyons, Lewis Research Center; Janice M. Margle, Pennsylvania State Univ., Abington, Pa. (on detail at Lewis Research Center under Intergovernmental Personnel Act; PO C-72822D). Presented at Combustion Institute Meeting, Cleveland, Ohio, May 5-6, 1986.

16. Abstract

Velocity profiles in vertical laminar diffusion flames were measured by using laser Doppler velocimetry (LDV). Four fuels were used: n-heptane, iso-octane, cyclohexane, and ethyl alcohol. The velocity profiles were similar for all the fuels, although there were some differences in the peak velocities. The data compared favorably with the theoretical velocity predictions. The differences could be attributed to errors in experimental positioning and in the prediction of temperature profiles. Errors in the predicted temperature profiles are probably due to the difficulty in predicting the radiative heat losses from the flame.

17. Key Words (Suggested by Author(s))	18. Distribution Statement
Combustion; Fire research; Velocity measurement; LDV; Flame velocity	Unclassified - unlimited STAR Category 34

19. Security Classif. (of this report)	20. Security Classif. (of this page)	21. No. of pages	22. Price*
Unclassified	Unclassified	12	A02

*For sale by the National Technical Information Service, Springfield, Virginia 22161

NASA-Langley, 1986